Direct determination of resonance phase shifts of soft x-ray diffraction in thin films by momentum-transfer-sensitive three-wave interference

H.-H. Wu,[1] Y.-R. Lee,[1] Y.-Y. Chang,[1] C.-H. Chu,[1] Y.-W. Tsai,[1] Y.-J. Liu,[1] C.-H. Hsieh,[2] L.-J. Chou,[2] and S.-L. Chang[1,*]

[1]*Department of Physics, National Tsing Hua University, Hsinchu, Taiwan 300, Republic of China*

[2]*Department of Materials Science and Engineering, National Tsing Hua University, Hsinchu, Taiwan 300, Republic of China*

(Received 29 July 2008; published 2 September 2008)

A method for direct determination of resonance phase shifts in a (001) CdTe/InSb thin-film system is developed using soft x-ray three-wave resonance diffraction. At the (002) Bragg peaks of CdTe and InSb, two inversion-symmetry related three-wave diffractions are systematically identified according to crystal symmetry and the resonance phase shifts versus photon energies are measured without turning the thin film upside down. The momentum-transfer selectivity at (002) reflections facilitates the quantitative determination of the phase shifts near the Cd L_3, Te L_3, and Sb L_2 edges.

DOI: 10.1103/PhysRevB.78.092101 PACS number(s): 61.05.cp, 07.60.Ly, 41.50.+h

I. INTRODUCTION

Resonance x-ray diffraction, utilizing the anomalous dispersion near the absorption edges of a constituent element, has recently become a powerful method for electronic and atomic structures characterization of materials[1–5] because absorption is closely linked to electronic transitions and diffraction itself reveals long-range ordering of crystalline solids. In the literature, resonant x-ray diffraction at three-wave geometry has proven to be capable of providing the information of phase shift due to resonance, which links the real parts of anomalous dispersion with the imaginary parts.[6] This could yield additional valence, empty orbital, and bonding information via the analysis of diffraction anomalous fine structure.[7] Moreover, the measurement of phase shifts at resonance could help to delineate charge/orbital ordering in highly correlated systems.

The three-wave resonance diffraction for phase measurements utilizes the fact that one of the diffracted waves serves as a reference for the other waves in the three-wave diffraction process and the interference between the two gives rise to intensity variation due to phase shifts at resonance. For quantitative analysis of phase, a pair of inversion-symmetry related (ISR) three-wave resonant diffractions is required. In other words, to fulfill the symmetry inversion, the crystal sample has to be turned upside down for the ISR diffraction to occur. This fact seems to limit the application of this three-wave resonant diffraction to only bulk single crystals. It is, however, known that thin films and nanostructured materials nowadays have widespread applications in micro/nanoelectronic, magnetic, optical components, and solar cells.[8–10] It is therefore most desired to apply this diffraction technique to directly measure resonance phase from thin-film systems and the like.

In this Brief Report, we develop an x-ray three-wave resonance diffraction method, which overcomes the sample orientation barrier and yet provides momentum-transfer sensitivity for phase measurements. Direct quantitative determination of the distributions of resonance phases near the Cd L_3, Te L_3, and Sb L_2 edges for a (001) CdTe/InSb thin-film system is reported.

II. X-RAY MULTIPLE DIFFRACTION EXPERIMENTS AT RESONANCE

Multiple-wave diffraction occurs when a single crystal is oriented in a position such that several sets of atomic planes simultaneously satisfy Bragg's laws for a single x-ray wave length. In other words, in the reciprocal space, several reciprocal-lattice points are simultaneously brought onto the surface of the Ewald sphere. For example, three-wave (*OGL*) diffraction [Fig. 1(a)] occurs when the crystal is first aligned to satisfy the Bragg's law of a *G* reflection—the primary reflection—and is then rotated around the reciprocal-lattice vector $\vec{g}$ of the *G* reflection—the azimuth ψ scan—to let the

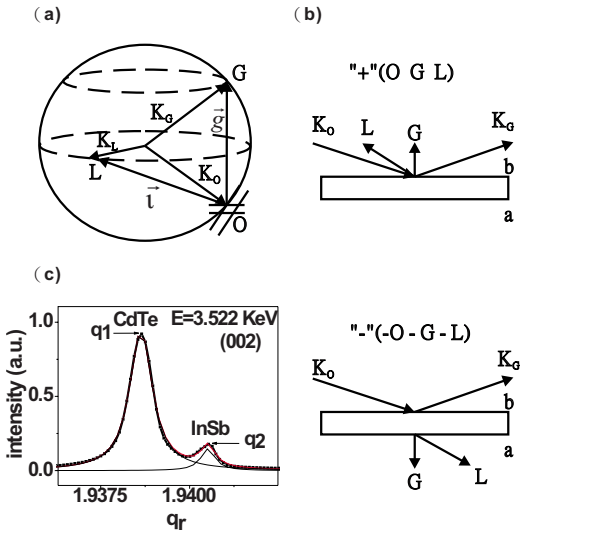

FIG. 1. (Color online) (a) Three-wave (*OGL*) diffraction geometry in the reciprocal space. $\vec{K}_O$, $\vec{K}_G$, and $\vec{K}_L$ are the wave vectors of the incident, primary reflected, and secondary reflected waves. Two sets of atomic planes of reciprocal-lattice vectors $\vec{g}$ and $\vec{l}$ are shown to satisfy the Bragg reflection simultaneously. (b) Inversion-symmetry related cases in real space. (c) The $\theta-2\theta$ scan of the primary reflection G(=002) of CdTe/InSb at the energy 3.522 keV, where q_r is the momentum transfer. The peaks of CdTe (002) and InSb (002) reflections occur at $q_r=q_1$(=1.9387 Å^{-1}) and q_2(=1.9405 Å^{-1}), respectively.

other reciprocal-lattice point L (the secondary reflection L) come onto the surface of Ewald sphere, thus, generating the secondary diffracted wave along the wave vector K_L. The intensity variation of the primary reflection G due to the interference between the primary reflected wave K_G and the secondary reflected wave K_L gives the phase information about the structure-factor triplet involved.[11–14] In addition, to enhance the interface sensitivity, we adopt the so-called Bragg-surface geometry,[15] where the wave vector K_L of the secondary reflected wave is parallel to the sample surface and the primary reflection G is a symmetric Bragg reflection.

Two ISR three-wave diffractions $[(O,G,L)$ and $(O,-G,-L)]$ are required for a quantitative estimation of triplet phases for single crystals [Fig. 1(b)],[11–14] where the crystal usually needs to be turned upside down when changing the diffraction geometry from (O,G,L) to $(O,-G,-L)$. To measure resonance phase shifts, the ISR diffractions are performed at various photon energies E covering the absorption edges of the constituent atoms.[1,11,12] The intensity modifications in the ψ scans around the reciprocal-lattice vectors of the primary reflections G and $-G$ are related to the triplet phases $\delta_{3\pm}$, where + and − represent the (O,G,L) and $(O,-G,-L)$ cases, respectively. Moreover, one half of the sum of the triplet phase δ_{3+} $(=-\delta_G+\delta_L+\delta_{G-L})$ of the structure-factor triplet $F_L F_{G-L}/F_G$ and δ_{3-} $(=-\delta_{-G}+\delta_{-L}+\delta_{L-G})$ of $F_{-L}F_{L-G}/F_{-G}$ is defined as the triplet resonance phase $\Delta[=(\delta_{3+}+\delta_{3-})/2]$. Far away from the absorption edges, the anomalous dispersion effect is negligibly small. The triplet resonance phase for an ISR Friedel pair [Fig. 1(b)] is almost zero. However, as the incident photon energy E is close to the absorption edge, the phase shift Δ has an appreciable magnitude due to a large anomalous dispersion.

The sample studied is a 500 Å thick (001) CdTe thin-film epitaxially grown on the (001) InSb substrate by molecular beams with lattice mismatch of only 0.05%.[16] At room temperature, the lattice constants are 6.482 and 6.476 Å for bulk CdTe and for InSb, respectively.

The experiments are carried out at the double-crystal monochromator (DCM) tender x-ray beamline 16A1 (1–9 keV) at the National Synchrotron Radiation Research Center in Taiwan. The vertical and horizontal acceptance angles and resolving power $E/\Delta E$ are 6, 0.5, and 7000 mrad, respectively. The resolution of the photon energy is 0.2 eV per step by tuning the Si(111) DCM. Because of the strong air absorption of soft x-rays, the whole experiment is held in a high-vacuum environment $(2\times10^{-7}$ torr) and an ultrahigh vacuum compatible six-circle kappa diffractometer[17] is used. Difficulty in performing the ISR diffraction for thin films is encountered because one cannot measure the diffracted intensity from the backside of the thin film without suffering heavy absorption from the thick substrate crystal. However, crystals having a zinc-blende structure with a four-fold axis symmetry along the [001] direction can be rotated around the [001] by 90° to produce a diffraction situation equivalent to the inverse diffraction case without turning the sample crystal upside down.[18] In other words, for an ISR three-wave diffraction, the primary reflection remains the same, i.e., $(00\bar{l})$ is equivalent to $(00l)$, while the secondary reflection changes from (hkl) to $(k\bar{h}l)$. This is because the 90° rotation around the $[00l]$ transforms (hkl) to $(k\bar{h}l)$ and the four-fold symmetry of $[00l]$ and the lattice symmetry yield the equivalence of $(00l)$ and $(00\bar{l})$. Hence, $(k\bar{h}\bar{l})$, the inversion of (hkl), is equivalent to $(k\bar{h}l)$. Therefore, two pairs of the ISR three-wave cases, $(000)(002)(1\bar{3}1)$ (denoted as "−") versus $(000)(002)(\bar{3}\bar{1}1)$ (denoted as "+") and $(000)(002)(331)$ (denoted as "−") versus $(000)(002)(3\bar{3}1)$ (denoted as "+"), are measured at photon energies covering the Cd L_3 and Te L_3 absorption edges, respectively, at the peak positions of CdTe (002) and InSb (002) whose momentum transfers are $q_1(=1.9387$ Å$^{-1})$ and $q_2(=1.9405$ Å$^{-1})$. Due to unavoidable overlap between the diffraction profiles for $E<4.28$ keV, the Te L_3 resonance diffraction is measured for $E\geq4.28$ keV, which also covers the Sb L_2 edge (4.38 keV).

According to the dynamical theory of x-ray diffraction,[11,14,19] the corresponding relative intensity distribution of three-wave diffraction I_G, proportional to the difference between the three-wave diffraction intensity $I_G(3)$ and two wave $I_G(2)$ of the primary reflection G,

$$I_G=[I_G(3)-I_G(2)]/I_G(2) \tag{1}$$

can be fitted by an asymmetrical Lorentzian function, consisting of symmetrical Lorentzian and Gaussian functions.[1]

$$L_\pm(\Delta\psi)=[a_\pm(\Delta\psi-\Delta\psi_\pm)-b_\pm]/[(\Delta\psi-\Delta\psi_\pm)^2+c_\pm^2], \tag{2}$$

where the symbols + and − represent (O,G,L) and $(O,-G,-L)$ cases, respectively. The triplet phases can be calculated from the adjusted fitting parameters $a_\pm$, $b_\pm$, and $c_\pm$, according to Eqs. (1)–(3), as

$$\tan\delta_{3\pm}=(b_\pm-b_\mp)/2a_\pm c_\pm. \tag{3}$$

Since the momentum transfer is given by $q_r=4\pi\sin\theta/\lambda=2\pi/d$, $q_1(=1.9387$ Å$^{-1})$ and $q_2(=1.9405$ Å$^{-1})$ [shown in Fig. 1(c)] are the momentum transfers for the (002) of CdTe and InSb, respectively. The ISR three-wave diffraction pair with the primary reflection at q_1 and q_2 will provide the phase information for that particular set of planes of the corresponding d. As can be seen in the upper panel of Fig. 2, the asymmetry of three-wave diffraction profiles of the "−" case labeled with open circles clearly changes when the photon energy E crosses the Cd L_3 edge at q_1. This implies changes of the triplet phases for E crossing the Cd L_3 edge while the profile asymmetries at q_2 almost keep the same even near the resonant state as shown in the lower panel of Fig. 2. Similar situation is also observed for the Te L_3 edge (not shown).

III. DETERMINATION OF PHASE SHIFTS DUE TO RESONANCE

The triplet and triplet resonant phases of all the ISR three-wave diffraction pair are determined according to Eqs. (2) and (3) for q_1 and q_2. Figures 3(a) and 3(b) show the measured triplet resonance phases Δ at q_1 and q_2 versus E in the vicinity of Cd L_3 and Te L_3, respectively. In Fig. 3(a), the q_1 curve labeled with solid squares shows nearly zero Δ value for E less than 3.538 keV; the Cd L_3 edge increases drasti-

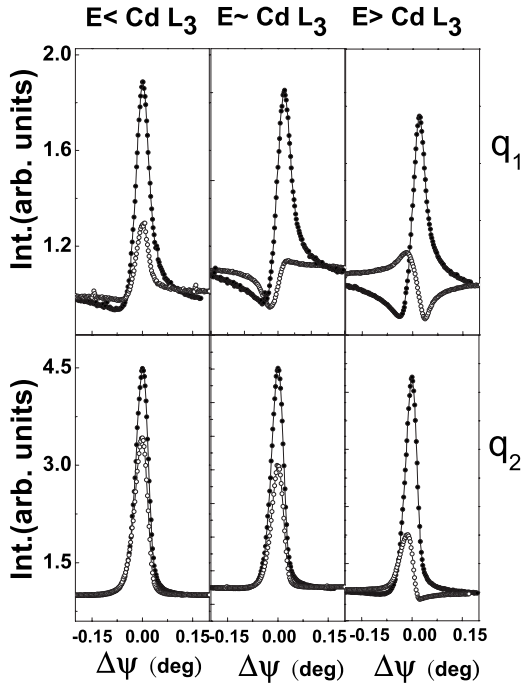

FIG. 2. Profiles in the upper panel display the three-wave intensities at energies crossing the Cd L_3 edge as the primary reflection is at q_1 position; similarly, profiles in the lower panel are intensities measured at q_2, respectively. The intensities are given in the unit of the two-wave intensity. Solid circles: (000)(002)($\bar{3}\bar{1}$1) "+" case; open circles: (000)(002)(1$\bar{3}$1) "−" case.

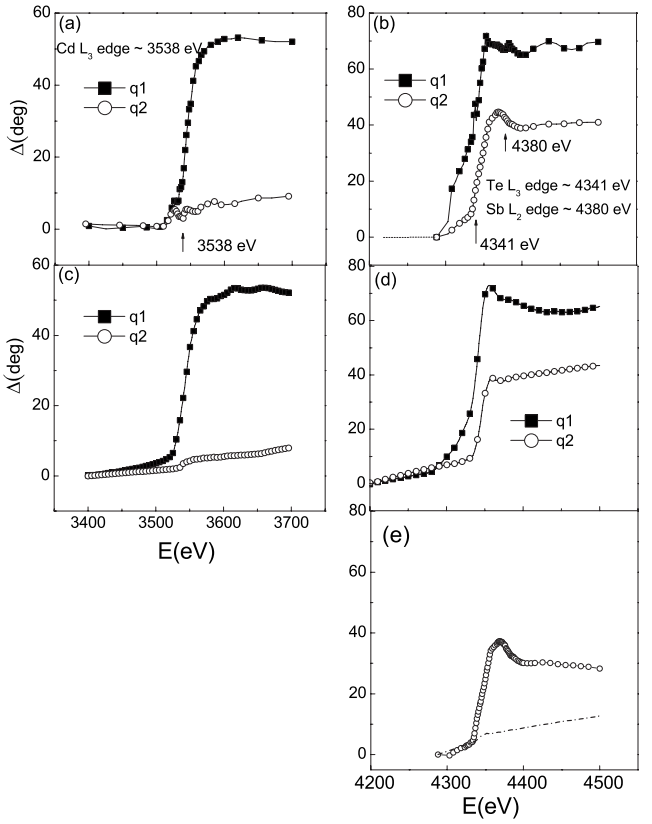

FIG. 3. (a) and (b) The triplet resonance phases versus the photon energies in the vicinity of the Cd L_3 and Te L_3 edges, respectively. (c) and (d) The calculated phases of (a) and (b) and the resonance phases (e) near the Sb L_2 edge (the open circles) and the calculated resonance phase curve for Te L_3 at $q_r=q_2$ (the dashed curve).

cally in the range of 30 eV above the edge and reaches a plateau of 50° afterwards. While the q_2 curve (with open circles) shows less pronounced increase, about 5°, after the edge and levels off for higher energies. This is because the q_1 curve is measured at the CdTe (002) peak position, which is more sensitive to the excitation of Cd than the q_2 curve measured at the InSb (002) reflection position. In other words, the anomalous dispersion effect detected due to Cd L_3 is more pronounced in the q_1 curve than in the q_2 curve. In Fig. 3(b), the q_1 curve behaves in a similar way as the q_2 curve [shown in Fig. 3(a)], except that the plateau is about 70° high. Although near the Te L_3 edge (4.341 keV), there is the Sb L_2 edge; the anomalous scattering due to Sb L_2 measured at q_1 is negligibly small compared to that due to Te L_3. Therefore, the q_1 curve represents the energy distribution of Δ due to the resonance near the Te L_3 edge. In contrast, the q_2 curve of Fig. 3(b) is not sensitive to Te L_3 but is very sensitive to the Sb L_2 anomalous scattering because the measurements are measured at the (002) InSb peak position. Hence, the anomalous scattering contribution from Te L_3 to the q_2 curve of Fig. 3(b) would be similar to the contribution from Te L_3 to the q_2 curve of Fig. 3(a), which can be simulated theoretically.

The calculated triplet resonance phases of CdTe and InSb for different energies near the Cd L_3 and Te L_3 edges are shown in Figs. 3(c) and 3(d), respectively. The dispersion correction f' and f'' of the atomic scattering factor extracted from the extended x-ray absorption fine-structure measurement are included in the theoretical calculation. The presence of Sb L_2 edge (4.38 keV) close to Te L_3 edge (4.341 keV) complicates the phase analysis. However, we could then calculate the resonance phase curve for Te L_3 at $q_r=q_2$ [the dashed curve in Fig. 3(e)] and subtract it from the q_2 curve of Fig. 3(b). This leads to the resonance phase curve (the open circles) for the resonance of Sb atoms at Sb L_2 shown in Fig. 3(e). As can be seen, the triplet resonance phase Δ has a peak value of about 40° at the Sb L_2 edge. The accuracy on the measured phases is estimated around ±5°. It should be noted that the anomalous scattering contributions from the In L_2 and In L_3 are nearly null because the two edges are located at 3.938 and 3.730 keV, respectively, which are out of the range of measurements for Te L and Sb L edges.

IV. DISCUSSION AND CONCLUSION

In conclusion, we have demonstrated the direct determination of resonance phase shifts near the Cd L_3, Te L_3, and Sb L_2 edges in CdTe/InSb thin-film system using momentum transfer to select the excitation of the CdTe thin film or InSb substrate in addition to photon energy tuning. In fact, this x-ray method stated here is capable of determining resonance phase for a variety of thin-film systems without restriction to any specific elements. Furthermore, since the secondary reflected wave propagates along the interface in the Bragg-

surface three-wave diffraction, abundant interface structural information is carried by this surface-diffracted wave, which should be useful for interface structure analysis. In fact, we did try to utilize the momentum-transfer sensitivity of this Bragg-surface resonance diffraction to determine the compositions of the interface between CdTe and InSb. Although the high-resolution transmission electron microscopy failed to identify the interface boundaries because of the proximity in atomic number between Cd and In and between Te and Sb, the measurement of the surface $(1\bar{3}1)$ diffraction according to Ref. 15 indicated negligibly small interface roughness. Under such circumstances, the preliminary results showed, qualitatively, the decrease in Cd and Te and increase in In and Sb concentrations along the interface normal toward the InSb substrate. Unfortunately, quantitative determination of interface concentration is not possible due to peak broadening in momentum-transfer measurements.

Although the diffraction peaks were rather sharp, indicating that the CdTe film is of good crystal quality, the resonance diffraction method proposed here is applicable to thin-film systems of less perfect crystallinity as long as the ISR three-wave diffraction profiles show distinct features irrespective of peak widths. Moreover, the phase analysis procedure is based on a Born approximation,[14] a kinematical approach, which is (in principle) valid to diffraction from less perfect-crystal systems.

ACKNOWLEDGMENTS

The authors are indebted to R. F. C. Farrow and T. C. Huang for providing the samples and to the Ministry of Education and National Science Council for their financial support.

*Author to whom correspondence should be addressed; slchang@phys.nthu.edu.tw

[1] Y. P. Stetsko, G.-Y. Lin, Y.-S. Huang, C.-H. Chao, and S.-L. Chang, Phys. Rev. Lett. **86**, 2026 (2001).
[2] T. L. Lee, R. Felici, K. Hirano, B. Cowie, J. Zegenhagen, and R. Colella, Phys. Rev. B **64**, 201316(R) (2001).
[3] I. S. Elfimov, N. A. Skorikov, V. I. Anisimov, and G. A. Sawatzky, Phys. Rev. Lett. **88**, 015504 (2001).
[4] Q. Shen, I. S. Elfimov, P. Fanwick, Y. Tokura, T. Kimura, K. Finkelstein, R. Colella, and G. A. Sawatzky, Phys. Rev. Lett. **96**, 246405 (2006).
[5] A. Qteish and R. J. Needs, J. Phys.: Condens. Matter **3**, 617 (1991).
[6] Y.-R. Lee, Yu. P. Stetsko, W.-H. Sun, S.-C. Weng, S.-Y. Cheng, G.-G. Lin, Y.-L. Soo, and S.-L. Chang, Phys. Rev. Lett. **97**, 185502 (2006).
[7] H. Stragier, J. O. Cross, J. J. Rehr, L. B. Sorensen, C. E. Bouldin, and J. C. Woicik, Phys. Rev. Lett. **69**, 3064 (1992).
[8] J. L. Loferski, J. Appl. Phys. **27**, 777 (1956).
[9] D. R. Yodershort, U. Debska, and J. K. Furdyna, J. Appl. Phys. **58**, 4056 (1985).
[10] L. Stolt, J. Hedstrom, J. Kessler, M. Ruckh, K.-O. Velthaus, and H.-W. Schock, Appl. Phys. Lett. **62**, 597 (1993).
[11] S.-L. Chang, H. E. King, M.-T. Huang, and Y. Gao, Phys. Rev. Lett. **67**, 3113 (1991).
[12] E. Weckert and K. Hummer, Acta Crystallogr., Sect. A: Found. Crystallogr. **53**, 108 (1997).
[13] Q. Shen, Phys. Rev. Lett. **80**, 3268 (1998).
[14] S.-L. Chang, *X-Ray Multiple-Wave Diffraction* (Springer-Verlag, Berlin, 2004).
[15] W.-C. Sun, H.-C. Chang, P.-K. Wu, Y.-J. Chen, C.-H. Chu, M.-T. Tang, Yu. P. Stetsko, M. Hong, and S.-L. Chang, Appl. Phys. Lett. **89**, 091915 (2006).
[16] A. T. S. Wee, Z. C. Feng, H. H. Hng, K. L. Tan, R. F. C. Farrow, and W. J. Choyke, J. Phys.: Condens. Matter **7**, 4359 (1995).
[17] T.-S. Gau, Y.-C. Jean, K.-Y. Liu, C.-H. Chung, C.-K. Chen, S.-C. Lai, C.-H. Shu, Y.-S. Huang, C.-H. Chao, Y.-R. Lee, C.-T. Chen, and S.-L. Chang, Nucl. Instrum. Methods Phys. Res. A **466**, 569 (2001).
[18] S.-L. Chang, Y.-S. Tsai, and M.-T. Huang, Phys. Lett. A **177**, 61 (1993).
[19] S.-L. Chang and M.-T. Tang, Acta Crystallogr., Sect. A: Found. Crystallogr. **44**, 1065 (1988).